

X-RAY FLARES AND OSCILLATIONS FROM THE BLACK HOLE CANDIDATE X-RAY TRANSIENT XTE J1650–500 AT LOW LUMINOSITY

JOHN A. TOMSICK¹, EMRAH KALEMCI², STÉPHANE CORBEL³, PHILIP KAARET⁴

Accepted by the Astrophysical Journal

ABSTRACT

We report on X-ray observations made with the *Rossi X-ray Timing Explorer* of the black hole candidate (BHC) transient XTE J1650–500 at the end of its first, and currently only, outburst. By monitoring the source at low luminosities over several months, we found 6 bright ~ 100 s X-ray flares and long time scale oscillations of the X-ray flux. The oscillations are aperiodic with a characteristic time scale of 14.2 days and an order of magnitude variation in the 2.8–20 keV flux. The oscillations may be related to optical “mini-outbursts” that have been observed at the ends of outbursts for other short orbital period BHC transients. The X-ray flares have durations between 62 and 215 s and peak fluxes that are 5–24 times higher than the persistent flux. The flares have non-thermal energy spectra and occur when the persistent luminosity is near $3 \times 10^{34} (d/4 \text{ kpc})^2 \text{ erg s}^{-1}$ (2.8–20 keV). The rise time for the brightest flare demonstrates that physical models for BHC systems must be able to account for the situation where the X-ray flux increases by a factor of up to 24 on a time scale of seconds. We discuss the flares in the context of observations and theory of Galactic BHCs and compare the flares to those detected from Sgr A*, the super-massive black hole at the Galactic center. We also compare the flares to X-ray bursts that are seen in neutron star systems. While some of the flare light curves are similar to those of neutron star bursts, the flares have non-thermal energy spectra in contrast to the blackbody spectra exhibited in bursts. This indicates that X-ray bursts should not be taken as evidence that a given system contains a neutron star unless the presence of a blackbody component in the burst spectrum can be demonstrated.

Subject headings: accretion, accretion disks — black hole physics: general — stars: individual (XTE J1650–500) — stars: black holes — X-rays: stars

1. INTRODUCTION

X-ray transients provide an opportunity to study accreting compact objects over a large range of luminosities and mass accretion rates. Until recently, most observations of black hole candidate (BHC) X-ray transients occurred when the sources were at very high luminosity ($\gtrsim 10^{36} \text{ erg s}^{-1}$) or very low luminosity ($\lesssim 10^{32} \text{ erg s}^{-1}$), and much less observing time was devoted to intermediate luminosities (see Chen, Shrader & Livio 1997 for a review of observations of X-ray transients). This situation has improved somewhat through observations with the *Rossi X-ray Timing Explorer* (Bradt, Rothschild & Swank, 1993) and also with imaging X-ray observatories. Over the past few years, we have been observing BHC transients during outburst decay with *RXTE*, the *Chandra X-ray Observatory* (Weisskopf et al., 2002), and also in the radio band (see, e.g., Tomsick & Kaaret 2000; Corbel et al. 2001; Tomsick, Corbel & Kaaret 2001; Kalemci 2002). One motivation for these observations is performing detailed studies of the transitions between the high-soft (or soft) and low-hard (or hard) spectral states (van der Klis, 1995) where significant changes in the X-ray spectral and timing properties occur. While these transitions typically occur at luminosities of about $10^{36} \text{ erg s}^{-1}$ (Nowak, 1995), our observing program is designed to extend to much lower luminosities as we have recognized that new phenomena associated with intermediate accretion rates may be found by observing in this rather poorly studied luminosity regime.

In the hard state for BHCs, it is likely that the X-ray emission is due to inverse Comptonization of soft photons by energetic electrons, but there is uncertainty about the system geometry and the mechanism for transferring energy to the electrons. One possibility is that the inner edge of the accretion disk recedes from the compact object in the hard state, leaving a hot, quasi-spherical, optically thin region in the inner portion of the accretion disk. Another possibility that implies a different site

for hard X-ray production and a different accretion geometry is that the hard X-ray emission is due to a large number of discrete regions above the accretion disk where magnetic reconnection events occur (Galeev, Rosner & Vaiana, 1979). While both of these possibilities describe physical processes that may occur in BHCs, neither provides a complete picture of accreting BHCs as radio observations in the hard state indicate the presence of a powerful compact jet (Fender, 2001). The compact jet has also been suggested as a possible contributor to the X-ray emission via inverse Comptonization or possibly a synchrotron mechanism (Markoff, Falcke & Fender, 2001; Markoff et al., 2003).

The BHC transient XTE J1650–500 was discovered in 2001 September when it was detected in the X-ray band in outburst by the *RXTE* All-Sky Monitor (ASM, Remillard, 2001). Pointed *RXTE* observations indicated X-ray spectral and timing properties typical of black hole systems: No X-ray pulsations were detected; the energy spectrum was consistent with a combination of a soft component, likely from the accretion disk, and a power-law component; and band-limited noise and quasi-periodic oscillations (QPOs) were observed (Markwardt, Swank & Smith, 2001; Revnivtsev & Sunyaev, 2001; Wijnands, Miller & Lewin, 2001). XTE J1650–500 was identified in the optical (Castro-Tirado et al., 2001) and also the radio (Groot, Tingay, Udalski & Miller, 2001), but the radio source was not resolved. XTE J1650–500 was observed in the X-ray band with *XMM-Newton* and *Chandra* during its outburst. The *XMM-Newton* spectrum represents one of the best examples of a smeared and gravitationally red-shifted iron $K\alpha$ emission line that has been detected for a stellar mass BHC (Miller et al., 2002). More recently, Homan et al. (2003) reported the detection by *RXTE* of a 250 Hz QPO, making XTE J1650–500 the sixth BHC where high frequency (>40 Hz) QPOs have been detected. Finally, optical observations near quiescence indicate a binary orbital period of 5.1 hr and an optical mass function of

$0.64 \pm 0.03 M_{\odot}$ (Sanchez-Fernandez et al., 2002). The value for the mass function is relatively low for a black hole system and could indicate that the system contains a relatively low mass black hole, has a low binary inclination ($i < 40^{\circ}$), or both.

During the 2001 X-ray outburst from XTE J1650–500, the source underwent dramatic changes in its X-ray spectral and timing properties. Generally, the changes were not unusual for BHC X-ray transients. The source started off in a hard state, with a hard energy spectrum and a high level of timing noise, made a transition to a soft spectral state, and then made a transition back to the hard state (Kalemci et al., 2003; Homan et al., 2003). Here, we focus on *RXTE* observations that were made well after the state transition when the source flux was between 10 and 100 times below the transition level. In §2, we describe the observations and our analysis of the data. We present the results of the analysis in §3. The results include the discovery of X-ray oscillations and flares, and we previously reported the oscillations in an IAU Circular (Tomsick et al., 2002). We discuss the results in §4 and summarize our conclusions in §5.

2. OBSERVATIONS AND ANALYSIS

We obtained 97 *RXTE* monitoring observations of XTE J1650–500 covering the end of its 2001–2002 outburst. These “Target of Opportunity” observations started on 2001 November 5 (MJD 52,218) and were triggered by the gradual drop in the X-ray flux that was observed by the *RXTE*/ASM. Of the 97 observations, 15 occurred prior to a 28 day gap caused by pointing restrictions related to the source position relative to the sun. Kalemci et al. (2003) report on timing analysis of these pre-gap observations, during which the 2.8–20 keV source rate was between 69 and 183 s^{-1} per PCU (Proportional Counter Unit), including counts from the top anode layer only. Here, we focus on the 82 post-gap *RXTE* observations that were made over a period of 182 days between 2001 December 22 and 2002 June 22. Immediately after the gap, the source rate had dropped to 21 s^{-1} , and for the remaining observations, the source rates averaged over the duration of each observation are shown in Figure 1a. The *RXTE* observations occurred approximately every 2 days with the exception of the time period between MJD 52,361 and MJD 52,385, during which there was only 1 observation. The exposure times for the 82 post-gap observations were between 384 and 3360 s with an average exposure time of 1516 s per observation. Long time scale (~ 14 day) and large-amplitude X-ray oscillations are apparent in the Figure 1a light curve.

For the light curve shown in Figure 1a and for much of the work described below, we used “Standard 2” PCA (Proportional Counter Array) data with 16 s time resolution and 129 energy channels. We extracted light curves and energy spectra using scripts developed at UC San Diego and the University of Tübingen that incorporate the standard software for *RXTE* data reduction (FTOOLS v5.2). We used the most recent (2002 February) release of the “Faint Source” model for background subtraction. Obtaining the best possible background subtraction is important for some aspects of this work because of the low source count rate. To achieve this, we used Standard 2 data from the top anode layer only and excluded data from PCU 0, which has a higher background level due to the loss of its propane layer⁵. The light curve shown in Figure 1a indicates that we obtain high quality background subtraction. For the final 8 observations, we detect little or no flux

⁵See <http://lheawww.gsfc.nasa.gov/users/craigm/pca-bkg/bkg-users.html> for a detailed analysis of the background model performance.

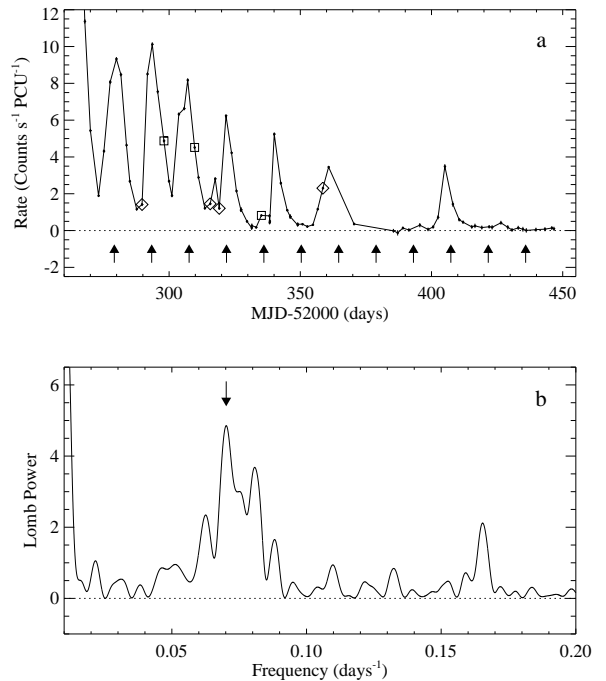


FIG. 1.— (a) The 2.8–20 keV PCA light curve at the end of the 2001 XTE J1650–500 outburst. The count rate is the background subtracted, top-layer rate for PCU 2. The diamonds mark observations during which X-ray flares occurred, and the squares mark the observations where simultaneous *Chandra* data were obtained. The rates shown include the counts from the X-ray flares. The arrows are spaced by 14.2 days. (b) The Lomb periodogram for the PCA light curve. The arrow marks the most significant peak in the periodogram, which is at 14.2 days, but it is not a periodic signal.

from XTE J1650–500, and the measured flux levels are consistent with the expected level from the Galactic ridge emission (Valinia & Marshall, 1998) in the PCA field of view for XTE J1650–500. Finally, we note that for some of the results described below, we used a second data mode with $125 \mu\text{s}$ time resolution that was obtained simultaneously with the 16 s time resolution data.

During 3 of the *RXTE* observations, we also obtained simultaneous observations with *Chandra* (on MJD 52,298, MJD 52,309 and MJD 52,335), and these are indicated in Figure 1a. Although we leave a detailed analysis of the *Chandra* data to a future paper, we refer to these observations in §3.3 and §3.5.

3. RESULTS

3.1. Discovery of X-Ray Flares

Through an inspection of the 16 s 2.8–20 keV PCA light curves for XTE J1650–500, we found that bright and isolated X-ray flares occurred during several of the *RXTE* observations. As shown in Figure 2, some of these flares show count rate increases by more than an order of magnitude over the persistent flux and durations near 100 s. Even though these flares are dramatic bursts of X-ray emission, significant variability is present in many of the other 16 s light curves. Thus, to ensure that we find the most extreme flares, we carried out a quantitative search for flares using the 16 s light curves. First, we produced a count rate histogram (i.e., the number of light curve time bins in various count rate ranges vs. count rate) for each observation. Then, we performed a least squares fit to these histograms with a Gaussian function. We obtained three parameters from the

fit: The Gaussian mean (r_{mean}); the width (σ); and the amplitude. For each observation, we calculated $x = (r_{max} - r_{mean})/\sigma$, where r_{max} corresponds to the maximum count rate in the 16 s light curve for that observation. Based on the number of observations and their duration, if the light curves contain only pure Gaussian noise, one expects approximately 1 observation with $x > 4$ and no observations with $x > 5$. In fact, for XTE J1650–500, 8 (out of 82) observations have $x > 7$, indicating the presence of a non-Gaussian component to the variability. It should be noted that, for light curves in general, a large value of x does not necessarily indicate the presence of flares because a long-term trend could also produce a large value of x . However, an inspection of the light curves for the 8 XTE J1650–500 observations with $x > 7$ indicates that these light curves contain large and rapid increases in flux (i.e., flares). In this work, we focus on the 5 observations that contain the most extreme flares with values of x between 10 and 20.

Closer examination of the flares in the 5 observations indicates that the properties of the flare that occurred during the observation on 2002 January 9 (MJD 52,283) are significantly different from those of the other flares. The Jan. 9 flare is extremely hard relative to the other flares. While the peak rate in the 2.8–20 keV band is similar for the flares in all 5 observations, the peak 20–60 keV count rate for the Jan. 9 flare is $18 \pm 1 \text{ s}^{-1}$ per PCU compared to non-detections in this energy band with upper limits of 1–2 s^{-1} per PCU for the other flares. In fact, there is good evidence that the Jan. 9 flare did not originate from any source within the *RXTE* field-of-view (FOV). Based on the PCA rates observed at the peak of the Jan. 9 flare, a source in the FOV should have been strongly detected with a count rate of approximately 600 s^{-1} in HEXTE (High-Energy X-ray Timing Experiment), which is the hard X-ray (20–200 keV) instrument that is co-aligned with the PCA on-board *RXTE* (Rothschild et al., 1998). We examined the HEXTE light curves for the Jan. 9 observation, and did not find any evidence for a count rate increase.

The properties of the Jan. 9 flare are very similar to 3 flares that were detected with *RXTE* during observations of other sources in 1998. The 1998 events have been attributed to X-rays and gamma-rays produced during solar flares⁶. To check the hypothesis that the Jan. 9 flare has a solar origin and that the other flares we detect during the XTE J1650–500 observations do not, we obtained publicly available X-ray light curves with 5 minute time resolution from one of the Geostationary Operational Environmental Satellites (GOES-12), which carries the Solar X-ray Imager (SXI). Very bright solar flares were detected with SXI at the time of the 2002 Jan. 9 flare and also at the times of the 1998 events. However, solar flares did not occur at the times of the other XTE J1650–500 flares, and we conclude that the Jan. 9 flare has a solar origin, but the other flares do not. Figure 2 displays PCA light curves with 4 s time resolution for the 4 XTE J1650–500 observations (henceforth, observations a-d) where we detect non-solar flares. We detect 6 flares (labeled 1–6 in Figure 2) in these observations and report on their detailed properties below.

3.2. Basic X-Ray Flare Properties

To characterize the flares, we extracted light curves for observations a-d with 1 s time resolution. Although PCA background estimates are only provided with 16 s time resolution, we used an interpolation procedure to background subtract the

⁶http://lheawww.gsfc.nasa.gov/users/keith/non_cosmic_bursts/burst_doc.html

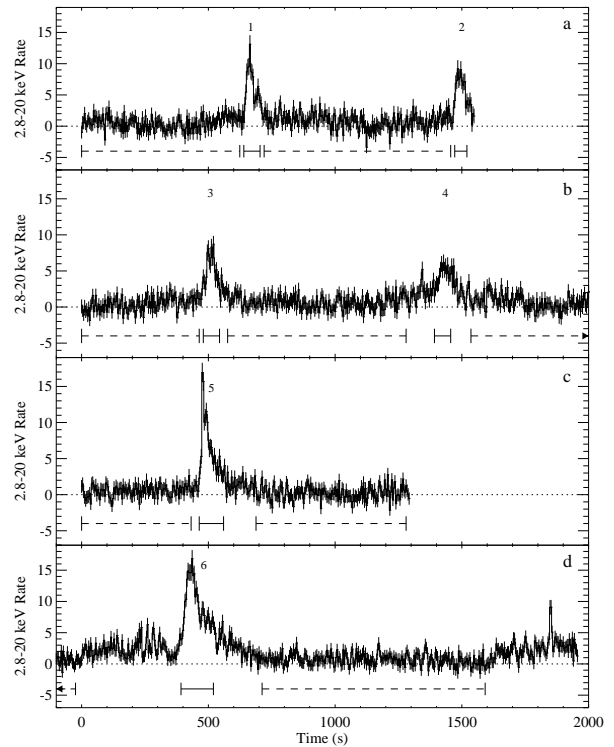


FIG. 2.— The 2.8–20 keV PCA light curves for the 4 observations where X-ray flares occurred. The time resolution is 4 s, and the light curves are background subtracted. To maximize the statistics, data from all PCUs that were on, including PCU 0, and all anode layers were used, but the rates are divided by the number of active PCUs to give counts $\text{s}^{-1} \text{PCU}^{-1}$. The flares are labeled 1–6, and the flare and non-flare times used for spectral analysis are marked with solid and dashed lines, respectively, below the light curves. The dates of the observations are (a) MJD 52289.7, (b) MJD 52315.7, (c) MJD 52319.1, and (d) MJD 52358.6.

1 s light curves. For each flare, we fitted the rise and decay with a function consisting of an exponential plus a constant. In most cases, an exponential does not provide a good description of the light curve if the peak of the flare is included, but acceptable fits are obtained when we include the portion of the light curve up to 85% of the flare peak. For the 12 fits (rises and decays for 6 flares), we obtain reduced χ^2 values between 0.81 and 1.54 with a mean reduced χ^2 of 1.07, typically for 110 degrees of freedom. Table 1 gives the e-folding rise and decay times for the 6 flares and also the flare durations. The durations are calculated using the exponential fits and defining the start of the flare to be the time when the rate rose to 20% above the constant level and the end of the flare to be the time when the rate reached 20% above the constant level during the decay. The results indicate that the flares have rise times of 3–18 s, decay times of 15–98 s, and durations of 62–215 s. For each flare, Table 1 also includes the ratio of the peak 2.8–20 keV count rate in the 4 s light curves to the non-flaring (i.e., persistent) rate in the same band. The non-flaring light curve regions are marked in Figure 2. The peak rates are 5–24 times higher than the persistent rates.

3.3. Flare and Non-Flare Energy Spectra

We studied the spectral properties for observations a-d, by producing 2.8–20 keV PCA energy spectra using data from the flare and non-flare times shown in Figure 2. We produced energy spectra for each flare individually and also a combined

spectrum with a 464 s integration time. We determined the non-flare times by inspection of the 16 s light curves and included all long, continuous segments where the count rate is relatively constant. We produced spectra for each of the 4 observations, and the exposure times for the non-flare spectra are given in Table 2. For spectral fitting, we used the XSPEC 11.2 software package. Based on fits to PCA energy spectra from observations of the Crab nebula that were contemporaneous with the XTE J1650–500 observations (see Tomsick, Corbel & Kaaret 2001 for a more detailed description of this procedure), we included 0.6% and 0.3% systematic errors for energy bins below and above 8 keV, respectively.

We fitted the 464 s flare spectrum with power-law and blackbody spectral models to determine if the flare emission mechanism is non-thermal or thermal. For these fits, we included interstellar absorption using the “phabs” model and left the column density (N_{H}) as a free parameter. Using the power-law model results in a very good fit with $\chi^2/\nu = 23/37$, while the result for the blackbody model is a poor fit with $\chi^2/\nu = 120/37$. Thus, it is clear that the flare spectrum is not dominated by a blackbody component. Furthermore, a two-component power-law plus blackbody fit does not provide a significant improvement over the power-law alone, and the upper limit on the blackbody contribution to the two-component fit is 7% of the total 2.8–20 keV flux.

The non-flare spectra are also well-described by a power-law model. However, for observations a and d, positive residuals appear between 6 and 7 keV that may indicate the presence of an iron $K\alpha$ emission line. For observation d, where the largest residuals occur, the line is consistent with being narrow and the line energy is 6.6 ± 0.3 keV. The equivalent width (EW) is poorly constrained to be between 200 eV and 1.4 keV (90% confidence). Based on the improvement in the quality of the fit when the line is included in the model, an F-test indicates that the line is required at only the 99.4% level. For the other non-flare observations and for the 464 s flare spectrum the 90% confidence EW upper limits are a few hundred eV or greater – consistent with the EW for observation d. Thus, for the spectral fits described below, we use a model consisting of a power-law and a narrow iron line.

For the flare and non-flare spectra, the power-law plus line spectral fits indicate that the constraints on the column density are poor, and we obtain 90% confidence upper limits on N_{H} in the range $(2\text{--}10) \times 10^{22}$ cm $^{-2}$. Our *Chandra* spectra (see §2) indicate a column density of about $N_{\text{H}} = 6 \times 10^{21}$ cm $^{-2}$, which is consistent with the PCA upper limits, the expected interstellar value (Dickey & Lockman, 1990), and also the values inferred from X-ray and optical observations obtained during outburst (Miller et al. 2002; Augusteijn et al. 2001; A. Castro-Tirado, private communication). We refitted the spectra after fixing N_{H} to the value we obtained from *Chandra*, and the results for the combined flare spectrum and the non-flare spectra are given in Table 2. While the combined flare spectrum does have a smaller best fit value for the power-law photon index (Γ) than the non-flare spectra, it is only marginally harder than the non-flare spectra for observations b and d. However, at $\Gamma = 1.59 \pm 0.08$ (90% confidence errors), the flare spectrum is significantly harder than the spectra of the two non-flare observations with the lowest flux, a and c, for which $\Gamma = 2.20^{+0.31}_{-0.26}$ and $\Gamma = 2.50^{+0.48}_{-0.43}$, respectively. This indicates that significant softening occurs at low flux levels, but it is not clear if this is related to the flaring behavior. We refitted the combined flare

spectrum after subtracting the average non-flare spectrum. This results in a slightly lower (harder) value for Γ , but the change in Γ is less than 0.1.

We also fitted the spectra for the individual flares and the values of Γ obtained are given in Table 1 along with the fluences for each flare. To determine the fluences, we first summed the total number of counts over the duration of the flare and subtracted the contribution from the persistent flux. We determined the start and end times for each flare as described in §3.2. We then used the spectral shape from fitting the individual flares to convert the total counts to a fluence in erg cm $^{-2}$.

3.4. Evolution of X-Ray Flare Properties

Figure 3 shows the light curves for the 6 flares in the hard (6.9–20 keV) and soft (2.8–6.9 keV) X-ray bands. While there are some specific light curve features that appear for only one of the energy bands, the main result is that there is good overall correlation between the soft and hard light curves. We also examined the hardness ratio vs. time using the hard and soft light curves, but the only obvious trend is that the flares are somewhat harder than the persistent emission, which is consistent with the spectral results reported in §3.3. For flare 6 especially, it is apparent that some of the specific light curve features are present for only one of the energy bands. During the rise of flare 6, near time = 400 s, there is an 8 s dip that only appears in the soft band light curve. Also, during the flare 6 decay (time = 465–540 s), oscillations with a ~ 20 s time scale are present in the hard band light curve only. In addition, flares 2 and 3 show some evidence for variability in the hard band that is not present in the soft band.

3.5. Long Time Scale Oscillations Observed with RXTE and Chandra

Here, we focus on the long time scale and large amplitude X-ray oscillations seen in Figure 1a. To determine the characteristic frequencies of the oscillation and to search for periodicities, we produced a Lomb periodogram (Press et al., 1992) of the time series, and it is shown in Figure 1b. The highest amplitude peak in the periodogram is at a frequency of 0.070 days $^{-1}$ (14.2 day period), but it is about a factor of 2 below the 3- σ detection limit for a periodic signal. The fact that there is excess power from 0.06 to 0.09 days $^{-1}$ suggests the presence of an aperiodic signal, and inspection of the light curve agrees with this conclusion. In Figure 1a, the arrows are spaced by 14.2 days, and while the first 4 peaks are consistent with this period, the agreement does not continue after MJD 52,330.

As the PCA is not an imaging instrument and has a relatively large field-of-view (1° radius), it is necessary to consider whether another source besides XTE J1650–500 could be responsible for the phenomena detected by the PCA. Thus, it is important that the *Chandra* observations mentioned in §2 firmly establish that XTE J1650–500 is the source of the oscillations. For all three *Chandra* observations, a source is strongly detected at the position of the XTE J1650–500 radio counterpart (Groot, Tingay, Udalski & Miller, 2001). The *Chandra* spectra are well-described by a power-law with interstellar absorption, and by fitting the spectra, we derive 0.5–10 keV fluxes of 5×10^{-11} erg cm $^{-2}$ s $^{-1}$ for the first two observations and 6×10^{-12} erg cm $^{-2}$ s $^{-1}$ for the third observation. Comparing these fluxes to the PCA count rates shown in Figure 1a indicates that the flux levels measured by *Chandra* and the PCA are well-correlated. As the *Chandra* observations prove that XTE

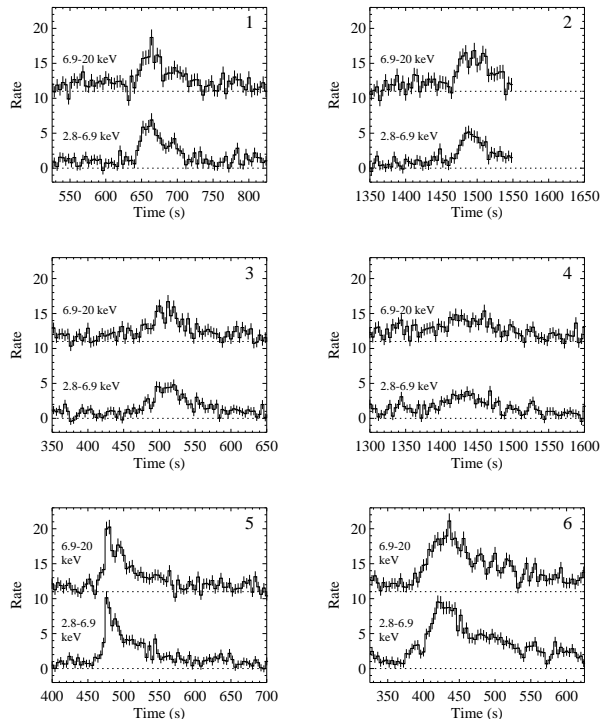


FIG. 3.— Light curves in 2 energy bands for the 6 X-ray flares. The time resolution is 4 s, and the light curves are background subtracted. To maximize the statistics, data from all PCUs that were on, including PCU 0, and all anode layers were used, but the rates are divided by the number of active PCUs to give counts $\text{s}^{-1} \text{PCU}^{-1}$. For each X-ray flare, the soft 2.8–6.9 keV band light curve is shown on the bottom. The hard 6.9–20 keV band light curve is shown on top and has been offset by 10 counts s^{-1} for clarity.

J1650–500 was still active when the flares were observed, it is very unlikely that the flares come from another source. Still, we used the SIMBAD database to search for X-ray sources in the PCA FOV, which is a 1° circle centered on the XTE J1650–500 position ($l = 336.70^\circ$, $b = -3.44^\circ$). We did not find any sources, such as X-ray binaries, that are likely to contribute significantly to the X-ray flux detected by the PCA. Further, the non-thermal flare spectrum rules out the possibility that the flares come from an X-ray burster in the PCA FOV (see §4.5 for more discussion of X-ray bursts).

4. DISCUSSION

During *RXTE* observations of the BHC XTE J1650–500, we have discovered 6 X-ray flares lasting from 62–215 s and peaking at count rate levels between 5 and 24 times the persistent rates. The flares occurred at the end of the first and currently only X-ray outburst that has been detected from this X-ray transient when the persistent flux was a factor of 10^3 below the peak flux level for the outburst. Although strong X-ray variability is commonly observed for black hole X-ray binaries, the isolated X-ray flares that we observe are unusual. In addition, we find long term aperiodic oscillations with a characteristic time scale of 14.2 days. Below, we discuss the implications of the XTE J1650–500 oscillations and X-ray flares by comparing them to phenomena that have been seen for other sources, including long and short time scale variability in black hole binaries, the X-ray flares that have been detected from Sgr A*, the super-massive black hole at the center of the Galaxy, and X-ray bursts in neutron star binaries.

4.1. XTE J1650–500 Oscillations

The fact that the ~ 14 day X-ray oscillations are an aperiodic phenomenon likely rules out the possibility that they are directly related to disk precession, and they are obviously not orbital since it is now known that XTE J1650–500 has an orbital period of 5.1 hr (Sanchez-Fernandez et al., 2002). However, oscillations have previously been observed in the optical at the ends of outbursts for a number of short orbital period BHC transients as well as dwarf novae (Kuulkers, 1998). The general properties of the optical oscillations can be explained in the framework of disk instability models (DIM) for dwarf novae (Osaki, Shimizu & Tsugawa, 1997; Hameury, Lasota & Warner, 2000) and possibly for X-ray transients (Menou et al., 2000). For DIM, the level of emission increases when the disk becomes hot enough for the hydrogen in the disk to be ionized. This leads to a higher viscosity and an increase in the mass accretion rate onto the compact object. Oscillations can be produced by the propagation of heating and then cooling waves through the disk (Hameury, Lasota & Warner, 2000). For BHC systems, the best examples of these optical oscillations (also called “mini-outbursts”) include GRO J0422+32 (Castro-Tirado et al., 1993; Chevalier & Ilovaisky, 1995), GRS 1009–45 (Bailyn & Orosz, 1995), and, more recently, XTE J1859+226 (Zurita et al., 2002). For XTE J1650–500, optical oscillations occurred contemporaneously with the X-ray oscillations we are reporting in this work (C. Bailyn, private communication). The optical oscillations have similar characteristic time scales of 10–100 days for all 4 sources. While X-ray coverage during optical oscillations was not obtained for GRS 1009–45 and was sparse for GRO J0422+32 and XTE J1859+226, the X-ray observations obtained for the latter 2 sources showed that they were active in the X-ray band during the oscillations (Shrader et al., 1997; Tomsick & Heindl, 2000). Another short orbital period BHC transient, 4U 1543–47, showed large variations in the X-ray band in a poorly sampled light curve obtained at the end of its 1971–1972 outburst (Chen, Shrader & Livio, 1997). Overall, the similarities between the XTE J1650–500 oscillations and those that have been seen for other short orbital period BHC transients suggests that they are related phenomena. If this is the case, our observations of XTE J1650–500 represent the first time that good X-ray coverage has been obtained during a series of mini-outbursts.

4.2. XTE J1650–500 X-Ray Flares and BHC Variability

While it is likely that the XTE J1650–500 oscillations are similar to phenomena that have been observed before (mostly in the optical band) for BHCs, it is not clear that the same can be said for the X-ray flares. In certain spectral states, BHC light curves certainly do exhibit a high level of variability, and their X-ray light curves contain flares that have inspired “shot noise” models (Terrell, 1972). However, in these models, it is the combination of a very large number of shots that can lead to the overall variability observed in BHCs, which can be as fast as millisecond time scales. The shots, and also the flares that are typically observed in BHC light curves, have much smaller amplitudes relative to the average flux levels and much shorter time scales than the XTE J1650–500 flares (see Miyamoto et al. 1992 for examples of light curves for other BHCs).

We found one example in the literature of a black hole system that exhibited a series of X-ray flares with some similarities to the XTE J1650–500 flares. V4641 Sgr is an unusual X-ray transient that was discovered in 1999 February by *RXTE* and

BeppoSAX. It is often referred to as a “fast” transient because it had an outburst in 1999 September that only lasted for about a day rather than the typical several months. The source showed extreme X-ray variability when it was bright, and, at the end of its most active period in 1999 September, it exhibited relatively isolated X-ray flares (Wijnands & van der Klis, 2000). Three or four X-ray flares occurred in a 200 s light curve shown in Figure 1c of Wijnands & van der Klis (2000). The X-ray flares had rise times < 10 s, durations of 20-50 s, flux increases by factors of 10-50 over the non-flaring flux, and roughly exponential decays at the ends of the flares. The similarities of the flare parameters and the fact that the flares for both V4641 Sgr and XTE J1650–500 occurred when the non-flaring flux was several orders of magnitude below the peak outburst flux for the respective sources leads us to suggest the possibility that the flares from the two sources could be related.

Although we do not believe that similar X-ray flares have been seen before in BHC sources other than XTE J1650–500 and possibly V4641 Sgr, this could partly be a selection effect. As discussed in §1, BHCs have been most often observed in outburst at high luminosity or in quiescence. From the optical observations of XTE J1650–500 that have been made (Sanchez-Fernandez et al., 2002; Augusteijn, Coe & Groot, 2001; Garcia & Wilkes, 2002), we estimate that the source distance is between 2 and 6 kpc, and here and below we use a fiducial value of 4 kpc for luminosity estimates. Thus, the typical non-flare X-ray flux of 1.7×10^{-11} erg cm $^{-2}$ s $^{-1}$ (2.8-20 keV, unabsorbed) corresponds to an luminosity of $3 \times 10^{34}(d/4 \text{ kpc})^2$ erg s $^{-1}$, which is in a luminosity regime where BHCs have not been as well-studied. Thus, we cannot rule out the possibility that X-ray flares commonly occur for BHCs at intermediate luminosities.

The fact that multiple X-ray flares are detected from XTE J1650–500 during observations a and b, suggests the possibility that XTE J1650–500 entered into a state (or perhaps an accretion regime) that favors flare production. It is interesting that the flares for observations a and b are both separated by 800-900 s, and this time scale may provide a clue about the flare emission mechanism. The observation d light curve also supports the idea that XTE J1650–500 enters into a flaring state since a short flare is seen at the end of that observation (near time = 1850 s). Furthermore, the *RXTE* observation following observation d (on MJD 52361) is one of the observations for which higher variability was detected, and short flares are also detected during that observation. Finally, a higher level of variability was detected for the *RXTE* observation that occurred between observations b and c on MJD 52318.

4.3. X-Ray Flares and Black Hole Accretion Theory

The XTE J1650–500 X-ray flares demonstrate that physical models for BHC systems must be able to account for the situation where the X-ray flux increases by a factor of up to 24 on a time scale of seconds (based on flare 5). While this time scale does not provide a useful model-independent constraint on the size of the emission region because the physical size of the system (i.e., the binary separation) is only a few light-seconds, we have considered whether the flares have implications for certain accretion scenarios. For flares produced by a change in mass accretion rate, the flux is expected to change on the viscous time scale in the X-ray emitting region of the accretion disk. For thin ($H \ll R$) and thick ($H \sim R$) accretion disks, where H is the accretion disk thickness and R is the radial distance from the compact object, the

viscous time scale is given by $t_v = \alpha^{-1}(R/H)^2 t_d$, where α is a dimensionless parameter that is proportional to the viscosity and t_d is the dynamical time scale (Frank, King & Raine, 1992). The dynamical (i.e., Keplerian) time scale depends on the mass of the compact object, M , and $R = rR_S$ ($R_S = 2GM/c^2$, where G is the gravitational constant and c is the speed of light) according to $t_d = 88 \mu\text{s} (M/M_\odot) r^{3/2}$. Based on the current distribution of black hole masses, it is likely that XTE J1650–500 contains a black hole with a mass of 5-15 M_\odot , and we assume a mass of 10 M_\odot . In the extreme case of $\alpha = 1$ (Frank, King & Raine, 1992) and a thick accretion disk ($R = H$), $t_v = 1$ s corresponds to $r = 110$, while a more realistic value of $\alpha = 0.1$ gives $r = 23$. Thus, if the flares are due to an increase in the mass accretion rate, they must originate in a region smaller than the inner ~ 20 -100 R_S of the accretion disk. While this does not strongly constrain theoretical models, the possibility of larger hard X-ray emission regions has been previously suggested (e.g., Esin, McClintock & Narayan 1997).

Some theoretical models for accreting black hole systems predict highly variable X-ray emission at low luminosities. Merloni & Fabian (2002) discuss the possibility of a “coronal outflow dominated accretion disk model,” where a geometrically thin and optically thick accretion disk dissipates much of its gravitational energy in a magnetic corona. This is an attractive model since it incorporates angular momentum transport via magnetic fields (Balbus & Hawley, 1991) and also the presence of outflows such as the compact jets that have been observed from accreting black holes at low luminosities (Fender, 2001). In this model, non-thermal X-ray flares can be produced through gradual magnetic field generation that can lead to a brightening of the corona (Merloni & Fabian, 2002). In another model that has been suggested for low luminosity black hole systems, the black hole accretes via a “hot settling flow” (Medvedev & Murray, 2002). Here, the black hole is magnetically coupled to the accretion flow, allowing a rapidly rotating black hole to transfer its angular momentum to the accretion flow as in Blandford & Znajek (1977). Hard X-ray spectra and high variability are expected for this accretion mode. In fact, Medvedev & Murray (2002) specifically predict that XTE J1650–500 may exhibit this behavior based on the spectral determination that it contains a rapidly rotating black hole (Miller et al., 2002).

4.4. Comparison between the X-Ray Flares in XTE J1650–500 and Sgr A*

Here, we consider the possibility that the XTE J1650–500 flares are related to the isolated X-ray flares that have been detected from Sgr A* (Baganoff et al., 2001; Goldwurm et al., 2003). Such a comparison is interesting because these are both low luminosity BHC or black hole systems, and the overall shapes of the flare light curves and the evolution of the energy spectra are similar in the two cases. For the Sgr A* flare seen by *Chandra* in 2000 October, the flux increases by a factor of about 45, and during the 10 ks flare, the X-ray spectrum hardens and is non-thermal (Baganoff et al., 2001). While the results for the 2000 October flare have been reported in the most detail, subsequent *Chandra* observations of Sgr A* yielded the detection of several more flares, and these suggest that flux increases by a factor of 5-25, similar to the XTE J1650–500 flares, are probably more typical (Baganoff et al., 2002). While the flare durations and rise times are about a factor of 100 less for XTE J1650–500 (durations of 100 s for XTE J1650–500 compared to 10 ks for Sgr A* and rise times of 10 s for XTE J1650–500

compared to 1 ks for Sgr A*), it is notable that the ratios for the two quantities are approximately the same. For *Chandra* observations of Sgr A*, the power-law photon index (Γ) is $2.2^{+0.5}_{-0.7}$ during non-flare times and $1.3^{+0.5}_{-0.6}$ during the 2000 October flare (Baganoff et al., 2001), which is consistent with the spectral evolution we observe for XTE J1650–500.

Although the phenomenology of the flares in Sgr A* and XTE J1650–500 have similarities, we must also consider the differences between these systems. Beyond the fact that the mass of the Sgr A* black hole is $2.6 \times 10^6 M_\odot$ (Eckart & Genzel, 1997) compared to the likely $\sim 10 M_\odot$ black hole in XTE J1650–500, the flares we observe for XTE J1650–500 occur when the persistent Eddington-scaled luminosity is much higher than for Sgr A*. For a distance of 4 kpc and a compact object mass of $10 M_\odot$, the persistent flux of $10^{-11} \text{ erg cm}^{-2} \text{ s}^{-1}$ for XTE J1650–500 (see Table 2) gives $L_x/L_{Edd} = 2 \times 10^{-5}$. For Sgr A*, the persistent X-ray luminosity is $2.2 \times 10^{33} \text{ erg s}^{-1}$ (Baganoff et al., 2001), indicating $L_x/L_{Edd} = 5 \times 10^{-12}$. Even if we consider the bolometric luminosity of $\sim 10^{37} \text{ erg s}^{-1}$ for Sgr A* (Narayan et al., 1998), $L/L_{Edd} = 2 \times 10^{-8}$, which is three orders of magnitude lower than XTE J1650–500. Thus, we consider the possibility that the flares in the two systems are related with the caveat that their accretion properties are likely to be significantly different.

If the flares are produced by similar processes, the fact that the flare time scales are longer for Sgr A* than for XTE J1650–500 is not surprising given the much larger black hole mass for Sgr A*. However, it is not obvious why the time scales would be different by only a factor of 100. For example, dynamical and viscous time scales at the same accretion disk radius, $r = R/R_S$, are proportional to the black hole mass. Thus, if the flares were produced by an increase in the mass accretion rate, the viscous time scale would be relevant (Liu & Melia, 2002), and a difference in time scale by a factor of 3×10^5 would be predicted. Baganoff et al. (2001) discuss the possibility that the Sgr A* flare emission could have a synchrotron or a synchrotron self-Compton (SSC) mechanism. This could occur if electrons were accelerated in magnetically active regions of an accretion flow (perhaps due to magnetic reconnection events). In these cases, the flare durations may be related to the synchrotron or SSC cooling time scales, which are proportional to $\gamma^{-1} B^{-2}$ (Begelman, Blandford & Rees, 1984), where γ is the Lorentz factor for the X-ray producing electrons and B is the magnetic field strength. The fact that the flare X-ray spectra are similar for Sgr A* and XTE J1650–500 may suggest that γ is not extremely different for the two systems, but, if B was an order of magnitude larger in the XTE J1650–500 emission region, then the predicted time scale would be a factor of 100 lower for this system, as observed. However, the calculations of di Matteo, Celotti & Fabian (1997) suggest that the difference in magnetic field strength should be much greater than an order of magnitude. Finally, jet-based models have been suggested to explain the Sgr A* flares (Markoff et al., 2001). In these models, the X-ray emission has a synchrotron or SSC mechanism, but the electrons are continuously shock accelerated so that the cooling time scales do not relate to the predicted flare duration in a simple way. More work is required to determine if any of these models can explain the time scale ratio of 100 between the XTE J1650–500 and Sgr A* flares.

4.5. X-Ray Flares and X-Ray Bursts

Accreting low magnetic field neutron stars exhibit type I X-ray bursts due to thermonuclear instabilities that result from ac-

cretion onto the neutron star surface (Lewin, van Paradijs & Taam, 1995). While XTE J1650–500 is a BHC and is not expected to produce type I X-ray bursts, the flare rise times, the decay times, and the ratio between the peak X-ray flux and the persistent flux are all typical of type I X-ray bursts (Lewin, van Paradijs & Taam, 1995). Even though the light curve shapes for the flares are typical of type I X-ray bursts, the spectral evolution is not. The emission mechanism for type I X-ray bursts is thermal, and X-ray bursts have energy spectra that are dominated by a blackbody component. As shown in §3.3, the possibility that the XTE J1650–500 X-ray flares have a significant blackbody component is strongly ruled out.

Although type II X-ray bursts are not as well understood and have only been detected from two sources to date, it is notable that some of the XTE J1650–500 flare light curves have properties similar to type II bursts. For flare 6, the variability leading up to the flare (time = 0–300 s in Figure 2), the dip right before the flare (time near 360 s), and the oscillations during the decay have similarities to the light curves of type II bursts (Lewin, van Paradijs & Taam, 1995; Lewin et al., 1996). However, like type I bursts, type II bursts also exhibit thermal spectra (Lewin, van Paradijs & Taam, 1995; Marshall et al., 2001) in contrast to the XTE J1650–500 flares. If XTE J1650–500 contains a black hole, then our conclusion that the X-ray flares are not type I or type II X-ray bursts indicates that X-ray bursts should not be taken as evidence for a neutron star in the system unless it can be shown that the burst energy spectrum is dominated by a blackbody component. This conclusion may have implications for estimates of the numbers of neutron star binaries in the Galaxy if a fraction of the putative X-ray bursters without high quality burst spectra actually contain black holes.

While the energy spectrum provides strong evidence against the XTE J1650–500 X-ray flares being X-ray bursts, we note that this possibility is also disfavored from luminosity considerations. Typically, peak X-ray burst luminosities are between $0.1 L_{Edd}$ and L_{Edd} . However, the flux at the peak of the XTE J1650–500 outburst is about 100 times higher than the peak of the strongest X-ray flare, indicating that if the X-ray flares are close to L_{Edd} , then the source was super-Eddington for most of the outburst, which seems implausible. In addition, given the observed flux, a peak X-ray flare luminosity of $0.1 L_{Edd}$ implies a distance between 28 kpc and 89 kpc for compact object masses between $1 M_\odot$ and $10 M_\odot$, and these large distances are ruled-out by the optical detections of the source near quiescence. However, these luminosity arguments may not be absolute proof against X-ray bursts because there are some unusual cases where bursts in other systems have been classified as type I X-ray bursts even though they are significantly sub-Eddington (e.g., Gotthelf & Kulkarni 1997; Garcia & Grindlay 1987). On the other hand, for the examples in the two preceding references, it has not been clearly demonstrated that non-thermal burst energy spectra are ruled out.

5. SUMMARY AND CONCLUSIONS

In this work, we report on *RXTE* observations of the BHC transient XTE J1650–500 made at the end of its first, and currently only, outburst. By observing at low luminosities, we found new or previously poorly studied X-ray phenomena, including bright ~ 100 s X-ray flares and long time scale oscillations of the X-ray flux. Over several months, the X-ray light curve shows strong aperiodic oscillations with a characteristic time scale of 14.2 days during which the X-ray flux varies

by an order of magnitude. We argue that the oscillations are probably related to the optical oscillations (also called “mini-outbursts”) that have been observed for other short orbital period BHC transients such as GRO J0422+32, GRS 1009–45, and XTE J1859+226. If this is the case, our observations represent the first time that good X-ray coverage has been obtained during a series of mini-outbursts.

A uniform analysis of the 16 s *RXTE* light curves leads to the detection of 6 X-ray flares in 4 observations with durations between 62 and 215 s and peak fluxes that are 5–24 times higher than the persistent flux. The flare energy spectra are non-thermal, being well-described by a power-law with a photon index of $\Gamma = 1.59 \pm 0.08$ (90% confidence errors). The upper limit on a blackbody contribution to the flare is 7% of the 2.8–20 keV flux. The flares are isolated events that occur when the persistent luminosity is low, near $3 \times 10^{34} (d/4 \text{ kpc})^2 \text{ erg s}^{-1}$ (2.8–20 keV), making them unusual, if not unique, for BHCs. The XTE J1650–500 X-ray flares demonstrate that physical models for BHC systems must be able to account for the situation where the X-ray flux increases by a factor of up to 24 on a time scale of seconds (based on flare 5). We briefly discuss two theoretical models for accreting black holes that predict highly variable X-ray emission at low luminosities (Merloni & Fabian, 2002; Medvedev & Murray, 2002).

We also compare the XTE J1650–500 flares to the X-ray flares that have recently been observed from Sgr A* by *Chandra* and *XMM-Newton* as these are both accreting black holes or BHCs that exhibited isolated X-ray flares during periods of low persistent luminosity (although we note that L_x/L_{Edd} and bolometric L/L_{Edd} are considerably lower for Sgr A*). The increases in flux and spectral evolution for the flares in the two systems are comparable, while the time scales (rise time and duration) are about 100 times faster for XTE J1650–500. Given the factor of $\sim 3 \times 10^5$ difference in compact object mass between the two systems (assuming that XTE J1650–500 contains a $10 M_\odot$ black hole), it is not surprising that the time scales are faster for XTE J1650–500. However, the simplest physical models suggest that the time scale difference should be considerably larger. Overall, we cannot rule out the possibility that the flares in the two systems are related, and more work is required on this topic.

Finally, we note that some of the XTE J1650–500 flares have light curves with similarities to type I X-ray bursts that are seen in neutron star systems, including rise times of seconds and exponential decays with e-folding times of tens of seconds. However, the non-thermal energy spectra for the flares are in contrast to the spectra of type I (and also type II) X-ray bursts, which are dominated by blackbody emission. Thus, the XTE J1650–500 flares indicate that X-ray bursts should not be taken as evidence for the presence of a neutron star in a given system unless the presence of a blackbody component can be demonstrated.

We would like to thank C. Bailyn for sharing results from optical observations of XTE J1650–500 ahead of publication. JAT acknowledges useful discussions with J. Miller, R. Hynes, A. Castro-Tirado, W. Yu, and F. Baganoff. SC acknowledges S. Markoff for stimulating discussions. We acknowledge useful comments and suggestions from an anonymous referee. The SIMBAD database and also information from the Space Environment Center, Boulder, CO, National Oceanic and Atmospheric Administration (NOAA), US Dept. of Commerce were used in preparing this paper. We would like to thank all sci-

entists who contributed to the Tübingen Timing Tools. JAT acknowledges partial support from NASA grant NAG5-10886 and Chandra award number GO2-3056X issued by the Chandra X-ray Observatory Center, which is operated by the Smithsonian Astrophysical Observatory for and on behalf of NASA under contract NAS8-39073. PK acknowledges partial support from NASA grant NAG5-7405. EK was partially supported by TÜBİTAK.

References

- Augusteijn, T., Coe, M., & Groot, P., 2001, IAU Circular, 7710
 Baganoff, F. K., et al., 2001, *Nature*, 413, 45
 Baganoff, F. K., et al., 2002, in American Astronomical Society Meeting 201, #31.08
 Bailyn, C. D., & Orosz, J. A., 1995, *ApJ*, 440, L73
 Balbus, S. A., & Hawley, J. F., 1991, *ApJ*, 376, 214
 Begelman, M. C., Blandford, R. D., & Rees, M. J., 1984, *Reviews of Modern Physics*, 56, 255
 Blandford, R. D., & Znajek, R. L., 1977, *MNRAS*, 179, 433
 Bradt, H. V., Rothschild, R. E., & Swank, J. H., 1993, *A&AS*, 97, 355
 Castro-Tirado, A. J., Kilmartin, P., Gilmore, A., Petterson, O., Bond, I., Yock, P., & Sanchez-Fernandez, C., 2001, IAU Circular, 7707
 Castro-Tirado, A. J., Pavlenko, E. P., Shlyapnikov, A. A., Brandt, S., Lund, N., & Ortiz, J. L., 1993, *A&A*, 276, L37
 Chen, W., Shrader, C. R., & Livio, M., 1997, *ApJ*, 491, 312
 Chevalier, C., & Ilovaisky, S. A., 1995, *A&A*, 297, 103
 Corbel, S., et al., 2001, *ApJ*, 554, 43
 di Matteo, T., Celotti, A., & Fabian, A. C., 1997, *MNRAS*, 291, 805
 Dickey, J. M., & Lockman, F. J., 1990, *ARA&A*, 28, 215
 Eckart, A., & Genzel, R., 1997, *MNRAS*, 284, 576
 Esin, A. A., McClintock, J. E., & Narayan, R., 1997, *ApJ*, 489, 865
 Fender, R. P., 2001, *MNRAS*, 322, 31
 Frank, J., King, A., & Raine, D., 1992, *Accretion Power in Astrophysics*, (Cambridge: Cambridge U. Press)
 Galeev, A. A., Rosner, R., & Vaiana, G. S., 1979, *ApJ*, 229, 318
 Garcia, M. R., & Grindlay, J. E., 1987, *ApJ*, 313, L59
 Garcia, M. R., & Wilkes, B. J., 2002, *The Astronomer’s Telegram*, #104
 Goldwurm, A., Brion, E., Goldoni, P., Ferrando, P., Daigne, F., Decourchelle, A., Warwick, R. S., & Predehl, P., 2003, *ApJ*, 584, 751
 Gotthelf, E. V., & Kulkarni, S. R., 1997, *ApJ*, 490, L161
 Groot, P., Tingay, S., Udalski, A., & Miller, J., 2001, IAU Circular, 7708
 Hameury, J., Lasota, J., & Warner, B., 2000, *A&A*, 353, 244
 Homan, J., Klein-Wolt, M., Rossi, S., Miller, J. M., Wijnands, R., Belloni, T., van der Klis, M., & Lewin, W. H. G., 2003, *ApJ*, 586, 1262
 Kalemci, E., 2002, Ph.D. Thesis, Temporal Studies of Black Hole X-Ray Transients During Outburst Decay
 Kalemci, E., Tomisick, J. A., Rothschild, R. E., Pottschmidt, K., Corbel, S., Wijnands, R., Miller, J. M., & Kaaret, P., 2003, *ApJ*, 586, 419
 Kuulkers, E., 1998, *New Astronomy Review*, 42, 1
 Lewin, W. H. G., Rutledge, R. E., Kommers, J. M., van Paradijs, J., & Kouveliotou, C., 1996, *ApJ*, 462, L39
 Lewin, W. H. G., van Paradijs, J., & Taam, R. E., 1995, in *X-ray Binaries*, eds. W.H.G. Lewin, J. van Paradijs & E.P.J. van den Heuvel (Cambridge: Cambridge U. Press), 175
 Liu, S., & Melia, F., 2002, *ApJ*, 566, L77
 Markoff, S., Falcke, H., & Fender, R., 2001, *A&A*, 372, L25
 Markoff, S., Falcke, H., Yuan, F., & Biermann, P. L., 2001, *A&A*, 379, L13
 Markoff, S., Nowak, M., Corbel, S., Fender, R., & Falcke, H., 2003, *A&A*, 397, 645
 Markwardt, C., Swank, J., & Smith, E., 2001, IAU Circular, 7707
 Marshall, H. L., et al., 2001, *ApJ*, 549, L167
 Medvedev, M. V., & Murray, N., 2002, *ApJ*, 581, 431
 Menou, K., Hameury, J., Lasota, J., & Narayan, R., 2000, *MNRAS*, 314, 498
 Merloni, A., & Fabian, A. C., 2002, *MNRAS*, 332, 165
 Miller, J. M., et al., 2002, *ApJ*, 570, L69
 Miyamoto, S., Kitamoto, S., Iga, S., Negoro, H., & Terada, K., 1992, *ApJ*, 391, L21
 Narayan, R., Mahadevan, R., Grindlay, J. E., Popham, R. G., & Gammie, C., 1998, *ApJ*, 492, 554
 Nowak, M. A., 1995, *PASP*, 107, 1207
 Osaki, Y., Shimizu, S., & Tsugawa, M., 1997, *PASJ*, 49, L19
 Press, W. H., Teukolsky, S. A., Vetterling, W. T., & Flannery, B. P., 1992, *Numerical recipes in FORTRAN. The art of scientific computing*, 2nd ed. (Cambridge: Cambridge U. Press)
 Remillard, R., 2001, IAU Circular, 7707
 Revnivtsev, M., & Sunyaev, R., 2001, IAU Circular, 7715
 Rothschild, R. E., et al., 1998, *ApJ*, 496, 538
 Sanchez-Fernandez, C., Zurita, C., Casares, J., Castro-Tirado, A. J., Bond, I., Brandt, S., & Lund, N., 2002, IAU Circular, 7989
 Shrader, C. R., Wagner, R. M., Charles, P. A., Harlaftis, E. T., & Naylor, T., 1997, *ApJ*, 487, 858
 Terrell, N. J. J., 1972, *ApJ*, 174, L35
 Tomisick, J. A., Corbel, S., & Kaaret, P., 2001, *ApJ*, 563, 229

- Tomsick, J. A., & Heindl, W. A., 2000, IAU Circular, 7456
Tomsick, J. A., & Kaaret, P., 2000, ApJ, 537, 448
Tomsick, J. A., Kalemci, E., Corbel, S., & Kaaret, P., 2002, IAU Circular, 7837
Valinia, A., & Marshall, F. E., 1998, ApJ, 505, 134
van der Klis, M., 1995, in X-ray Binaries, eds. W.H.G. Lewin, J. van Paradijs & E.P.J. van den Heuvel (Cambridge: Cambridge U. Press), 252
Weisskopf, M. C., Brinkman, B., Canizares, C., Garmire, G., Murray, S., & Van Speybroeck, L. P., 2002, PASP, 114, 1
Wijnands, R., Miller, J. M., & Lewin, W. H. G., 2001, IAU Circular, 7715
Wijnands, R., & van der Klis, M., 2000, ApJ, 528, L93
Zurita, C., et al., 2002, MNRAS, 334, 999

TABLE 1
BASIC FLARE PROPERTIES

Flare Number	MJD ^a -52,000 (days)	Rise Time ^b (s)	Decay Time ^b (s)	Duration ^b (s)	Count Rate Increase ^c	Γ^d	Fluence ^e
1	289.69046	7 ± 3	25 ± 6	65 ± 11	12.4 ± 1.4	1.92 ^{+0.29} _{-0.27}	2.8 × 10 ⁻⁹
2	289.70009	4.2 ± 1.6	17 ± 4	62 ± 7	8.7 ± 1.3	1.62 ^{+0.29} _{-0.27}	2.7 × 10 ⁻⁹
3	315.65935	13 ± 4	15 ± 4	67 ± 9	8.2 ± 1.1	1.51 ^{+0.29} _{-0.27}	2.5 × 10 ⁻⁹
4	315.67009	18 ± 10	33 ± 11	118 ± 24	5.8 ± 1.0	1.63 ^{+0.35} _{-0.30}	2.9 × 10 ⁻⁹
5	319.11676	2.9 ± 0.6	37 ± 5	75 ± 8	23.5 ± 1.8	1.68 ^{+0.21} _{-0.20}	3.9 × 10 ⁻⁹
6	358.59491	18 ± 3	98 ± 8	215 ± 14	15.6 ± 1.3	1.61 ^{+0.13} _{-0.12}	1.2 × 10 ⁻⁸

^aModified Julian Date at the peak of the X-ray flare.

^bSee text for precise definition.

^cRatio of the peak count rate in the 4 s light curves to the persistent 2.8-20 keV rate.

^dPower-law photon index for the flare energy spectra with 90% confidence errors.

^e2.8-20 keV burst fluence in erg cm⁻² for the duration of the flare.

TABLE 2
FLARE AND NON-FLARE ENERGY SPECTRA

Obs.	F/NF ^a	Exposure ^b (s)	Γ^c	Flux ^d
a-d	F	464	1.59 ± 0.08	1.09 × 10 ⁻¹⁰
a	NF	1392	2.20 ^{+0.31} _{-0.26}	1.47 × 10 ⁻¹¹
b	NF	1712	1.75 ^{+0.24} _{-0.22}	1.67 × 10 ⁻¹¹
c	NF	1056	2.50 ^{+0.48} _{-0.43}	9.61 × 10 ⁻¹²
d	NF	1088	1.72 ^{+0.31} _{-0.28}	1.69 × 10 ⁻¹¹

^aFlare (F) or non-flare (NF).

^bExposure time included in the spectra.

^cPower-law photon index for the energy spectra with 90% confidence errors.

^d2.8-20 keV absorbed flux in erg cm⁻² s⁻¹.